Journal of Inflammation Research

Dovepress
Taylor & Francis Group

Open Access Full Text Article

ORIGINAL RESEARCH

Sex Differences and Androgen Regulation Shape Mucosal Immune Phenotype, Gut Microbiota, and Microbiota-Derived Lactate in SKG Arthritis Model

Xinran Wu[1,*], Lingjuan Jiang[2,3,*], Yubin Cao[2], Peng Wang[2], Wenjing Wang[2], Xuan Zhang[1]

[1]Department of Rheumatology and Immunology, Beijing Hospital, National Center of Gerontology, Institute of Geriatric Medicine, Chinese Academy of Medical Sciences & Peking Union Medical College, Beijing, 100730, People's Republic of China; [2]State Key Laboratory of Complex Severe and Rare Diseases, Peking Union Medical College Hospital, Chinese Academy of Medical Sciences & Peking Union Medical College, Beijing, 100730, People's Republic of China; [3]Center for Biomarker Discovery and Validation, National Infrastructures for Translational Medicine, Institute of Clinical Medicine, Peking Union Medical College Hospital, Chinese Academy of Medical Sciences & Peking Union Medical College, Beijing, 100730, People's Republic of China

*These authors contributed equally to this work

Correspondence: Lingjuan Jiang; Xuan Zhang, Email irisjlj@163.com; zxpumch2003@sina.com

Objective: This study aimed to investigate the role of sex differences and androgen regulation in the development of arthritis, focusing on their effects on gut microbiota, metabolic profiles, and immune responses in the SKG mouse model of arthritis.

Methods: Eight-week-old male and female SKG mice were injected with zymosan to explore sex-related differences in arthritis progression. Androgen regulation was assessed in 4-week-old male SKG mice through castration and sham surgeries. Flow cytometry, 16S rDNA sequencing, metabolomics, histopathology, and immunofluorescence were used to evaluate immune responses, microbiota composition, and metabolic alterations.

Results: Sex differences significantly impacted immune cell composition, particularly dendritic cells (DCs), in the mesenteric and popliteal lymph nodes. Male mice exhibited an increased proportion of conventional type I DCs (cDC1), while female mice displayed a higher proportion of conventional type II DCs (cDC2). Androgen deprivation in male mice worsened disease severity, with reduced cDC1 cells and increased inflammatory infiltration. Sex differences also influenced gut microbiota, with higher levels of Lactobacillus in females, and castrated males resembling females in microbiota composition. Metabolomic analysis revealed significant sex-related differences, with lactate showing the most pronounced androgen-related changes. Additionally, androgen regulated hypoxia inducible factor-1 alpha (HIF1α) expression in mucosal DCs, promoting an immune tolerance phenotype.

Conclusion: This study highlights the significant role of sex and androgen regulation in arthritis development, revealing complex interactions between hormones, microbiota, and immune regulation. These findings suggest new avenues for sex-specific therapeutic strategies and precision interventions targeting microbiota and metabolic modulation in arthritis and other autoimmune diseases.

Keywords: arthritis, androgen regulation, dendritic cells, gut microbiota, microbiota-derived lactate, immune tolerance

Introduction

Rheumatoid arthritis (RA) is a chronic autoimmune disorder with an unclear etiology. It is characterized by progressive joint inflammation, pain, and deformities. In advanced stages, these manifestations can lead to functional disability, severely impairing patients' quality of life.[1] RA is characterized by a significant sex disparity in prevalence, with females exhibiting a markedly higher incidence—approximately two to three times that of males.[1] Previous studies suggest that sex hormones, mainly estrogen and androgen, play a crucial role in the sexual dimorphism observed in RA susceptibility.[2,3] However, the downstream mechanisms by which sex factors influence immune regulation in arthritis pathogenesis are not fully understood. Accumulating evidence suggests significant sexual dimorphism in the gut microbiota composition.[4] As a vital interface between the external environment and the host's internal environment, alterations in gut microbial composition, known as dysbiosis, have been identified as key environmental factors closely linked to arthritis development.[5–9] The gut microbiota

Received: 11 July 2025
Accepted: 30 October 2025
Published: 14 November 2025

plays a crucial role in the mucosal immune system, interacting with immune cells in the gut to maintain both local homeostasis and systemic immune balance.[10] Moreover, specific bacterial taxa in the gut microbiota regulate immune responses by degrading dietary macromolecules and producing metabolites or vesicles that function as signaling molecules, interacting with immune cells and displaying distinct immunomodulatory properties depending on microbial abundance.[11–14] When the gut microbiota undergoes compositional changes, immune cells in the gut, such as DCs, respond to microbial-derived metabolic signals. This leads to the activation or suppression of immune responses. These changes are transmitted through the gut-joint axis, ultimately influencing the phenotype of arthritis.[15–17] Given these findings, sex-related differences in gut microbiota composition may influence host immune responses. However, research on the role of sex-specific gut microbiota differences and microbiota-derived metabolites in arthritis pathogenesis has not been fully explored.

To explore these dynamics, we aim to investigate the role of sex in modulating arthritis phenotypic differences through the gut microbiota using SKG arthritis-prone mice.[18] By comparing disease progression in male and female SKG model mice, as well as in male mice undergoing orchiectomy (androgen depletion), following induction with zymosan, we analyzed the composition of the gut microbiota and its related metabolites, along with the accompanying immune cell changes. Our results offer new insights into the complex interactions among sex, gut microbiota, and metabolic factors and the immune system in the context of arthritis pathogenesis.

Methods

Mice and Disease Induction

SKG mice were obtained from Clea Japan. These mice were maintained in a specific-pathogen-free (SPF) facility throughout the experimental period. All research protocols were approved by the Animal Ethics Committee of Peking Union Medical College Hospital. The animal ethics committee approval number is XHDW-2023-054. The SKG mouse model of arthritis was initiated by injecting zymosan (Sigma-Aldrich, Z4250) intraperitoneally at a dose of 2 mg per mouse when they were 6 weeks old. Throughout the experiment, disease activity scores and body weights of the SKG mice were regularly monitored. Upon completion of the study, the SKG mice were euthanized in a humane manner. Arthritis severity was assessed using clinical scores as outlined in Supplementary Table 1.[9]

Androgen-Deprivation Surgery

4-week-old male SKG mice were randomly assigned to either the castration group or the sham-operation group for the androgen-deprivation surgical procedure. Prior to surgery, mice were anesthetized by intraperitoneal injection of pentobarbital sodium at a dose of 50 mg/kg. In the castration group, the testes were removed after disinfection of the surgical site, while in the sham-operation group, no testicular excision was performed to serve as a control for the surgical procedure itself. This surgery imposed certain traumatic stress on mice. Mice that die within two weeks post-surgery will be excluded from the study. Following a 2-week postoperative observation period, at 6 weeks of age, each SKG mouse in both groups received an intraperitoneal injection of 2 mg of the zymosan solution to induce arthritis. After inducing arthritis, photographs were taken of the hind-paw joints, mesenteric lymph nodes (MLN), and popliteal lymph nodes (PLN) to document the morphological changes. Colon and joint tissue samples were also collected for histological evaluation.

Histopathology

The lower-limb joints and colon tissues from SKG mice model were fixed in 4% paraformaldehyde, embedded in paraffin, sectioned, and stained with hematoxylin and eosin (HE). Pathologists, blinded to the group assignments, scored the samples based on criteria from Supplementary Table 2 for joint pathology[9] and Supplementary Table 3 for intestinal pathology.[19]

Flow Cytometry

The MLN and PLN tissues of SKG mice were dissected at the experimental endpoint. The tissues were ground thoroughly to dissociate the cells, and the resulting cell suspension was passed through a 100-μm cell filter to obtain a single-cell suspension. After that, the cells were blocked with TruStain FcX PLUS anti-mouse CD16/32 (BD Pharmingen cat.553141) at 4 °C for

10 minutes. The blocked cells were stained with LIVE/DEAD dye (Biolegend cat. 423105) to label dead cells, followed by staining with AF700 anti-mouse CD45 (Biolegend cat.103128), APC anti-mouse CD11c (Biolegend cat.117310), PE anti-mouse CD11b (Biolegend cat. 101208), BV421 anti-mouse MHCII (Biolegend cat. 107632), AF488 anti-mouse CD103 (Biolegend cat. 121408), and BV605 anti-mouse Ly-6G (Biolegend cat.117310) for 30 minutes. After staining, the cells were washed and resuspended in phosphate-buffered saline (PBS) containing ethylenediaminetetraacetic acid (EDTA) and bovine serum albumin (BSA). Flow cytometry was performed using an Invitrogen Attune NxT flow cytometer. The flow cytometry gating strategy followed Supplementary Figure 1A, and acquired data were analyzed with FlowJo software (Version 9).

16S rDNA Sequencing Detection

Fecal samples were collected from the colorectal segment of SKG mice at the end of the experiment. Genomic DNA was extracted from the feces using the QIAamp PowerFecal Pro DNA Kit. The preparation of DNA libraries and subsequent shotgun metagenomic sequencing were conducted by Biomarker Technologies Co., Ltd., Beijing, China. Specific primers with Barcodes were synthesized based on full-length primer sequences to amplify the 16S rDNA region of bacterial genomes in the fecal samples. PCR amplification was performed, and the resulting products were purified, quantified, and normalized to create a sequencing library (SMRT Bell). Sequencing of marker genes was carried out using the single-molecule real-time sequencing method on the PacBio platform. The CCS sequences were denoised and processed using the dada2 method in QIIME2 2020.6 software to obtain ASVs. Taxonomic annotation of the feature sequences was done using the SILVA reference database and the alignment method with the naive Bayes classifier. Community composition of each sample was analyzed at different taxonomic levels, and species abundance tables were generated using QIIME software. R-language tools were used to create visual community structure diagrams at each taxonomic level.

Metabolomics Detection

Cecal content samples from SKG mice were collected at the end of the experiment for combined detection of MRM300 and short-chain fatty acids.

For MRM300 analysis by LC-MS/MS, the samples were weighed under low-temperature conditions to prevent metabolite degradation. An extraction solution was added to the samples, followed by grinding, sonication, and a 1-hour incubation. After centrifugation at 12000 rpm and 4°C for 15 minutes, the supernatant was transferred to an injection vial. LC-MS/MS analysis was performed using an Agilent 1290 Infinity II UHPLC with an ACQUITY UPLC BEH C18 column. A SCIEX Triple Quad 6500+ mass spectrometer was used for mass spectrometry in MRM mode. Data acquisition and quantitative analysis were conducted with SCIEX Analyst Work Station Software (1.7.32) and BIOTREE Bio Bud (v2.0.3) automated analysis software.

For the analysis of short-chain fatty acids by GC-MS, the samples were vortexed and sonicated to release the short-chain fatty acids. After centrifugation, the supernatant was transferred to a new tube and an internal-standard extraction solution was added. The mixture was vortexed, oscillated, and sonicated in an ice-water bath. After centrifugation and cooling, the supernatant was transferred to an injection vial. Analysis was done using a Shimadzu GC2030-QP2020 NX gas chromatography-mass spectrometer with an Agilent HP-FFAP capillary column. Data acquisition and quantitative analysis were completed using GCMSsolution (4.50) and BIOTREE Bio Bud (v2.0.3) software.

Immunofluorescence

Colorectal tissues from mice were collected at the end of the experiment. The tissues were fixed in 4% paraformaldehyde, embedded in paraffin, and sectioned. The sections were deparaffinized in xylene, rehydrated in alcohol, and underwent antigen retrieval. Subsequently, the sections were blocked with 5% goat serum and incubated overnight at 4 °C with primary antibodies (HIF1α, 1:400, CST 48085S; CD11c, 1:100, Abcam ab219799). After washing to remove unbound primary antibodies, secondary antibodies were added and incubated at room temperature. The sections were washed again to remove unbound secondary antibodies, and the nuclei were stained with DAPI. After staining, the sections were washed, fixed, and mounted. Three random fields of each sample were selected at random and photographed under 20× magnification. Images were acquired using Pannoramic 250 FLASH Slide Scanner Systems and CaseViewer was used for image analysis.

Isolation and Culture of Primary Bone Marrow-Derived Dendritic Cells (BMDCs)

Bone marrow cells were isolated from the femurs of C57BL/6 mice for the differentiation of BMDCs. For bone marrow cell culture, RPMI-1640 medium supplemented with 10% fetal bovine serum (FBS) and 1% penicillin-streptomycin was used. Cells were grown in 6-well plates at a density of 4×10^6 cells/mL per well in the presence of 20 ng/mL granulocyte-macrophage colony-stimulating factor (GM-CSF, PeproTech) and 20 ng/mL Interleukin 4 (IL-4, PeproTech). Cultures were maintained for 7 days. On day 7, cells were harvested and stimulated with 100 ng/mL lipopolysaccharide (LPS, Sigma-Aldrich), with concurrent treatment with D-lactic acid sodium (10 mM, Sigma-Aldrich) or dihydrotestosterone (DHT, 10 nM, AbMole) alongside LPS. ddH_2O was used as the vehicle control. After 24 hours of stimulation, cell supernatants were collected, and Interleukin 6 (IL-6) secretion was detected by ELISA (MULTI SCIENCES).

Data Statistics

Data are presented as mean ± standard deviation (SD). Joint scores and body weights of mice were analyzed by two-way analysis of variance (ANOVA) using GraphPad Prism 10 software. Multiple group comparisons were conducted using Šídák's multiple comparisons test. When no significant interaction was observed between factors, Student's *t*-test was applied for analyses of pathological scores and cell ratios. Statistical significance was defined as $P < 0.05$.

Results

Sex Difference in Murine Models of Arthritis Impacted the Immune Cell Composition in the Lymph Nodes in the Intestine and Joints

To investigate the impact of sex on the development of the arthritis, we used 6-week-old male and female SKG mice, inducing disease onset (as shown in Figure 1A), and tracked the progression of arthritis phenotypes across sex. Following disease induction, female mice started to exhibit differences from male mice on the 28th day. Female mice showed significantly higher disease activity scores in their joints compared to male mice (Figure 1B), with no statistical difference in body weight between the two groups (Figure 1C). Pathologically, the ankle joints of female mice were more prominently swollen, and redness and swelling were observable in the metacarpophalangeal joints (Figure 1D). Both the MLN and PLN of female mice were affected, with their volumes visibly increased upon macroscopic inspection (Figure 1E). HE staining and pathological score demonstrated that the intestines and joints of female mice presented more severe inflammatory infiltration, along with synovial hyperplasia (Figure 1F and G). Furthermore, female mice showed an increase in DCs and cDC2 in the MLN. In contrast, the proportion of cDC1, a cell type associated with regulatory and tolerogenic function,[20] decreased in female mice but was upregulated in male model mice (Figure 1H and I). A similar trend was also observed in the PLN (Figure 1J and K). In comparison to DCs, macrophages and neutrophils exhibited differences in the MLN of male and female mice, but these differences did not extend to the PLN (Supplementary Figure 1B–E).

Collectively, these findings indicate that the arthritis phenotype and the distribution of immune cells within the lymph nodes are influenced by sex differences. In male model mice, there was an increase in cDC1 in the gut and joint-associated lymph nodes.

Androgen Associated with the Increase of cDC1s in SKG Mouse Model of Arthritis

To systematically investigate whether the increased cDC1 in the gut and joint-associated lymph nodes of male model mice is related to sex hormones, we performed androgen deprivation in the SKG mouse model of arthritis. This involved performing castration and sham operations on immature (4-week-old) male SKG mice. Two weeks after the surgeries, arthritis was induced in the SKG mice by injecting zymosan, and the changes in arthritis phenotype were observed (Figure 2A). The clinical scores of castrated male mice were higher than those of sham-operated mice (Figure 2B), with no statistically significant variance in body weight seen between the two groups (Figure 2C). Castrated male mice experienced more severe joint swelling and had visibly larger MLN and PLN (Figure 2D and E), and showed increased inflammatory infiltration and tissue damage in colon and joint tissues and histological scoring than the control group (Figure 2F and G). Flow cytometry was used to analyze immune cells in the MLN and PLN. The ratios of DC cells, cDC2 cells, macrophages, and neutrophils showed no significant differences between castrated and sham-operated male mice. However, cDC1 cells were significantly reduced in castrated male mice in both the MLN and PLN (Figure 2H–K and Supplementary Figure 2A–D).

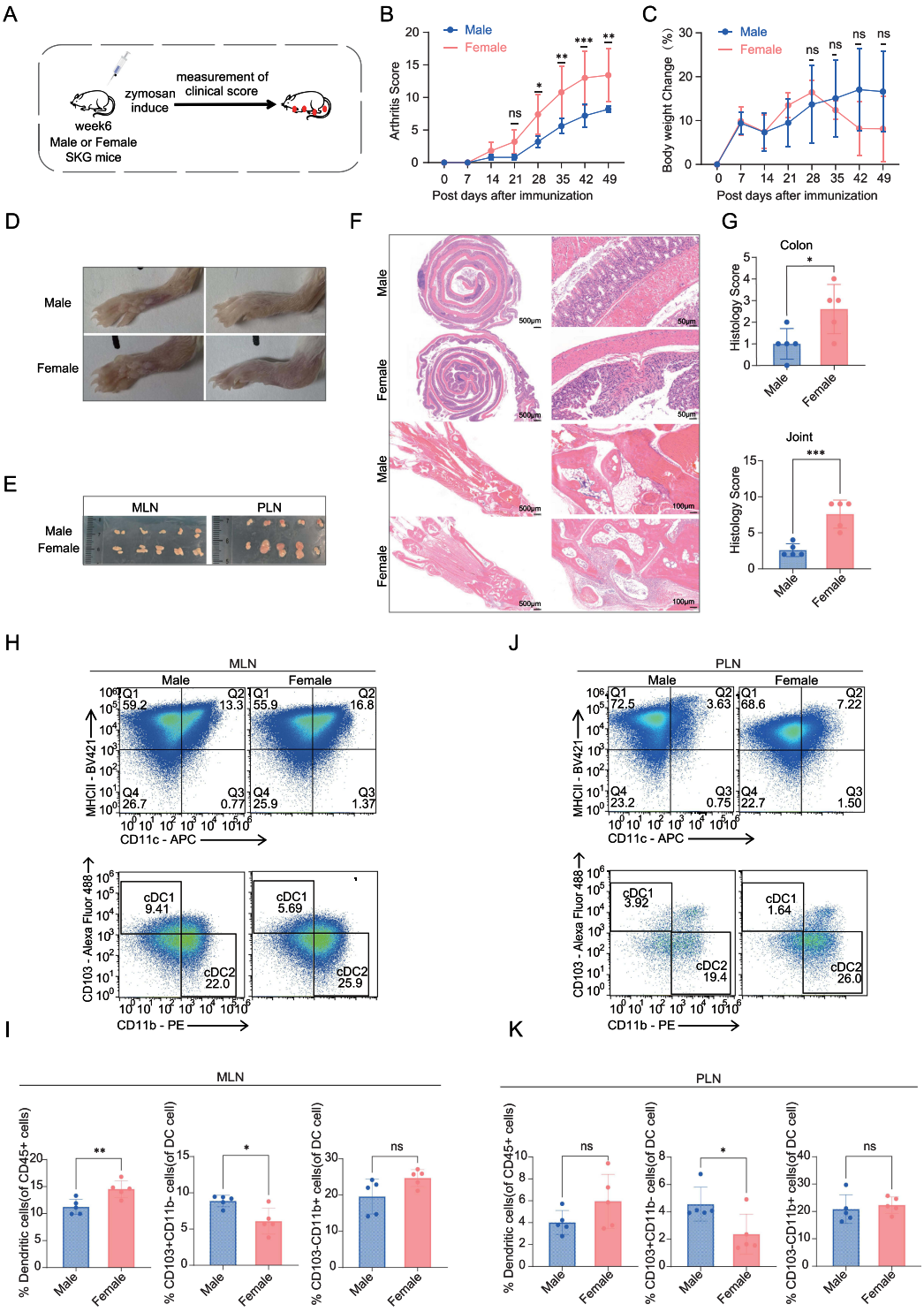

Figure 1 Sex difference affected the immune cell composition in murine lymph nodes of intestine and joints. (**A**) Schematic diagram of zymosan-induced disease onset in female and male SKG mice. (**B**) Temporal changes in arthritis clinical scores for female (n=5) and male (n=5) SKG mice. Time effect: p<0.0001, Sex effect: p<0.0001, Interaction: p =0.0036. (**C**) Body weight changes in female (n=5) and male (n=5) SKG mice. Time effect: p=0.4515, Sex effect: p<0.0001, Interaction: p =0.9603. (**D**) Photographs of the hind-paw joints in female and male SKG mice, covering finger and ankle joints. (**E**) Photographs of MLN and PLN from female and male SKG mice. (**F**) HE-stained images of SKG mice's colon and joint tissues (Scale bar = 500μm). (**G**) Pathological scores for colon and synovial tissues. (**H** and **I**) Changes in the composition of DCs in the MLN of female and male SKG mice. Representative flow cytometry plots (**H**) and quantification (**I**) show the proportions of total DCs (CD11c+MHCII+), cDC1 (CD103+CD11b$^-$) and cDC2 (CD103+CD11b$^-$) subsets. (**J** and **K**) Changes in the composition of DCs in the PLN of female and male SKG mice. Representative flow cytometry plots (**J**) and quantification (**K**) show the proportions of total DCs, cDC1 and cDC2 subsets. Results are presented as mean ± SD for (**B, C, G, I** and **K**). Each point represents data from one sample. *P*-values were calculated using two-way ANOVA for (**B** and **C**) and the Student's s *t*-test for (**G, I** and **K**). The statistical significance values are indicated as: *p < 0.05, **p < 0.01, ***p < 0.001.

Abbreviation: ns, not significant.

https://doi.org/10.2147/JIR.S552491

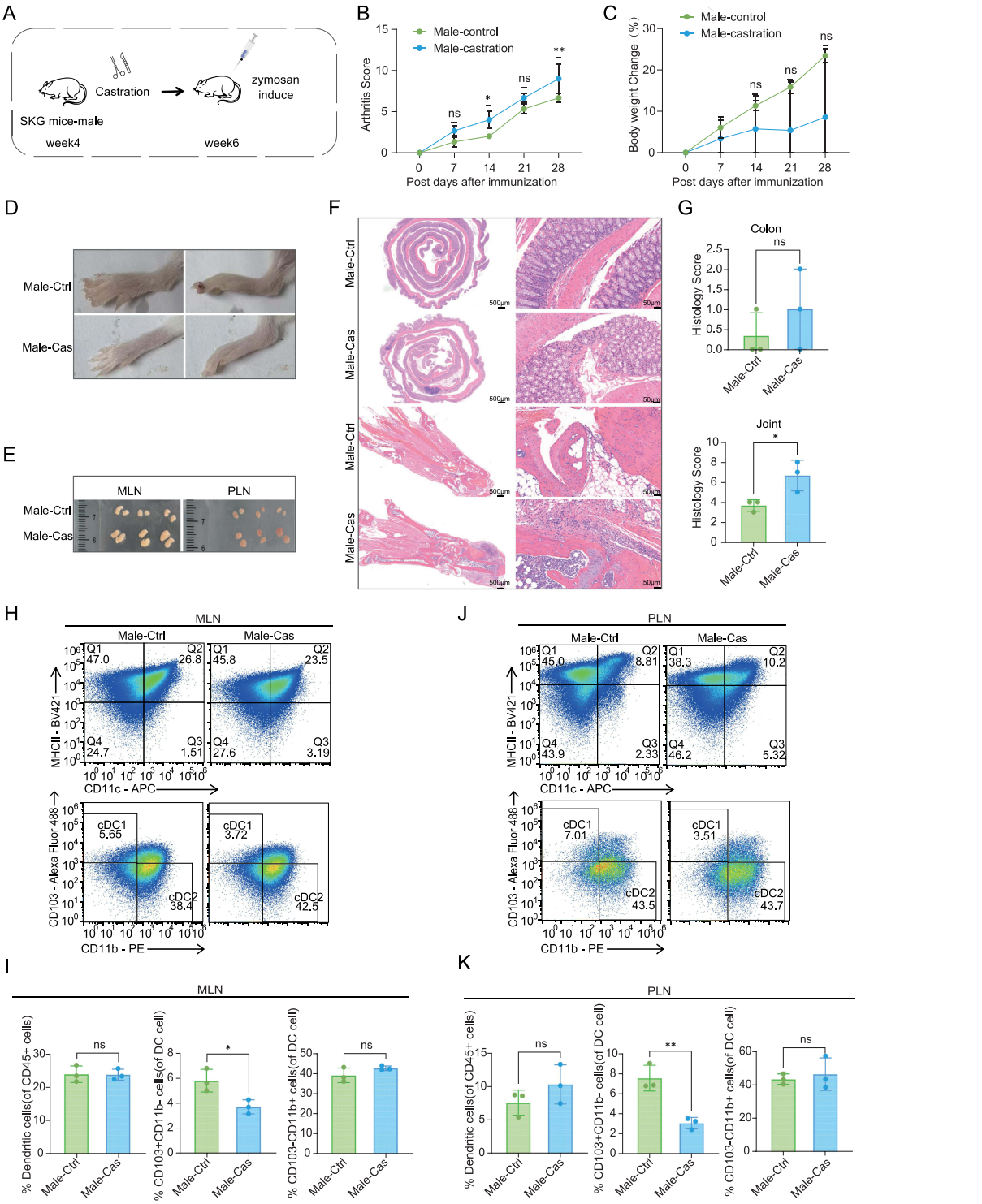

Figure 2 Androgen associated with the increase of cDC1s in SKG mouse model of arthritis. (**A**) Schematic of zymosan-induced arthritis in male SKG mice, comparing the castrated and sham-operated groups. (**B**) Temporal changes in clinical arthritis scores for sham-operated (n=3) and castrated (n=3) mice. Time effect: p<0.0001, Sex effect: p<0.0001, Interaction: p =0.1163. (**C**) Body weight variations in sham-operated (n=3) and castrated (n=3) mice. Time effect: p=0.0061, Sex effect: p=0.0120, Interaction: p =0.0061. (**D**) Representative images of hind paws, including finger and ankle joints, from both groups. (**E**) Photographs of MLN and PLN from sham-operated and castrated mice. (**F**) HE-stained images of colon and joint tissues from the sham-operated and castration groups (Scale bar=500 μm). (**G**) Pathological scores for colon and synovial tissues. (**H** and **I**) Changes in the composition of DCs in the MLN of sham-operated and castrated mice. Representative flow cytometry plots (**H**) and quantification (**I**) show the proportions of total DCs (CD11c+MHCII+), cDC1 (CD103+CD11b$^-$) and cDC2 (CD103+CD11b$^-$) subsets. (**J** and **K**) Changes in the composition of DCs in the PLN of sham-operated and castrated mice. Representative flow cytometry plots (**J**) and quantification (**K**) show the proportions of total DCs, cDC1 and cDC2 subsets. Each symbol in (**G, I** and **K**) represents an individual animal. Error bars indicate mean ± SD for (**B, C, G, I** and **K**). Statistical significance was determined using two-way ANOVA for (**B** and **C**) and the Student's *t*-test for (**G, I** and **K**). *P < 0.05, **P < 0.01.

Abbreviation: ns, not significant.

These findings indicate that fluctuations in androgen levels affect cDC1 in the lymph nodes, which in turn modulates the arthritis phenotype.

Sex Factors Influenced the Microbiota Composition in the SKG Mouse Model of Arthritis

Considering the sex difference associated with immune cells in both MLN and PLN, as well as the potential impact of alterations in gut microbiota on immune cells in the SKG model of arthritis,[21] we are curious about the interplay between sex difference and gut microbiota in the context of arthritis. Therefore, we conducted 16S rDNA sequencing to analyze the gut microbiota composition of the SKG model of arthritis and operation groups.

Principal coordinate analysis (PCoA) based on microbial composition and Bray-Curtis distance analysis revealed significant differences in fecal microbial composition between sexes (PERMANOVA, R^2 = 0.281, P-value = 0.009; Figure 3A). Female and male SKG mice exhibited distinct abundances of major bacterial genera (Figure 3B). Further analysis using linear discriminant analysis effect size (LEfSe) indicated that in fecal samples of male and female mice model, *Lactobacillus, Limosilactobacillus*, and related species (eg, *Lactobacillus johnsonii* and *Limosilactobacillus reuteri*) were more prevalent in female mice (higher LDA Score) (Figure 3C). Post-surgery, a difference in fecal microbial composition was observed between the two groups (PERMANOVA, R^2 = 0.365, P-value = 0.001; Figure 3D). Variations in the proportions of multiple genera were also detected among individual castrated and sham-operated male mice model (Figure 3E). Specifically, *Lactobacillus*, which were previously abundant in female mice, were found to be more prevalent in castrated male SKG mice, while the family *Bacteroidaceae* and the genus *Bacteroides* were relatively enriched in control (sham-operated) male mice (Figure 3C and F).

Collectively, these data suggest that sex appears to influence microbiota composition in SKG model. Both female mice and castrated male mice exhibited similar microbial changes when compared to male model mice.

Sex Factors Influenced the Gut Metabolites, with Androgen Being Associated with the Increase of Lactate in the SKG Model of Arthritis

Sex plays a crucial role in shaping the gut microbiota of SKG mice, which may influence the types and amounts of gut metabolites. To gain insight into how gut microbiota-derived metabolites affect the physiological state of SKG model mice, cecal contents were collected for metabolomics analysis. Principal component analysis (PCA) indicated a clear separation between female and male SKG mice (Figure 4A). Moreover, a larger number of metabolites showed differential expression in male mice. The top five up-regulated metabolites in male mice were 4-Aminohippuric acid, Indoxylsulfate, O-Phosphoethanolamine, 3-Guanidinopropionic acid, and Glycerophosphoric acid (Figure 4B). Additionally, there was a distinct separation between castrated male SKG mice and sham-operated male SKG mice (Figure 4C), with the five most significantly up-regulated metabolites in sham-operated males being Homogentisic acid, Phenylacetylglycine, Cinnamoylglycine, Lactic acid, and 3-Hydroxyisobutyric acid (Figure 4D). By intersecting the differential metabolites identified in the two compared groups, we discovered 13 differential metabolites. These substances showed differences between male and female SKG mice, as well as between castrated and sham-operated male SKG mice, indicating their sensitivity to androgen influence (Figure 4E). Notably, lactic acid exhibited the most significant androgen-related change (Figure 4F).

The findings suggest that sex hormones have an influence on the alterations in gut metabolites in SKG mice. The removal of androgen leads to a significant change in gut lactate levels in SKG mice compared to the sham-operated male group, highlighting the impact of androgen on lactate levels in the gut.

Androgen Regulated Gut Lactate and Mucosal Tolerance Cells Related to Lactate

Given that androgens are linked to immune phenotypes[22] and modulate gut microbiota and metabolite expression,[23] we further investigated the regulatory effects of androgens—along with lactate—on dendritic cells (DCs) via in vitro assays. LPS-stimulated BMDCs were co-cultured with D-lactic acid sodium and dihydrotestosterone (DHT) for 24 hours, and culture supernatants were collected and analyzed (Figure 5A). Both D-lactic acid sodium and DHT reduced IL-6 secretion by LPS-stimulated BMDCs (Figure 5B). Recent studies indicate that lactate activates HIF-1α in DCs in the experimental

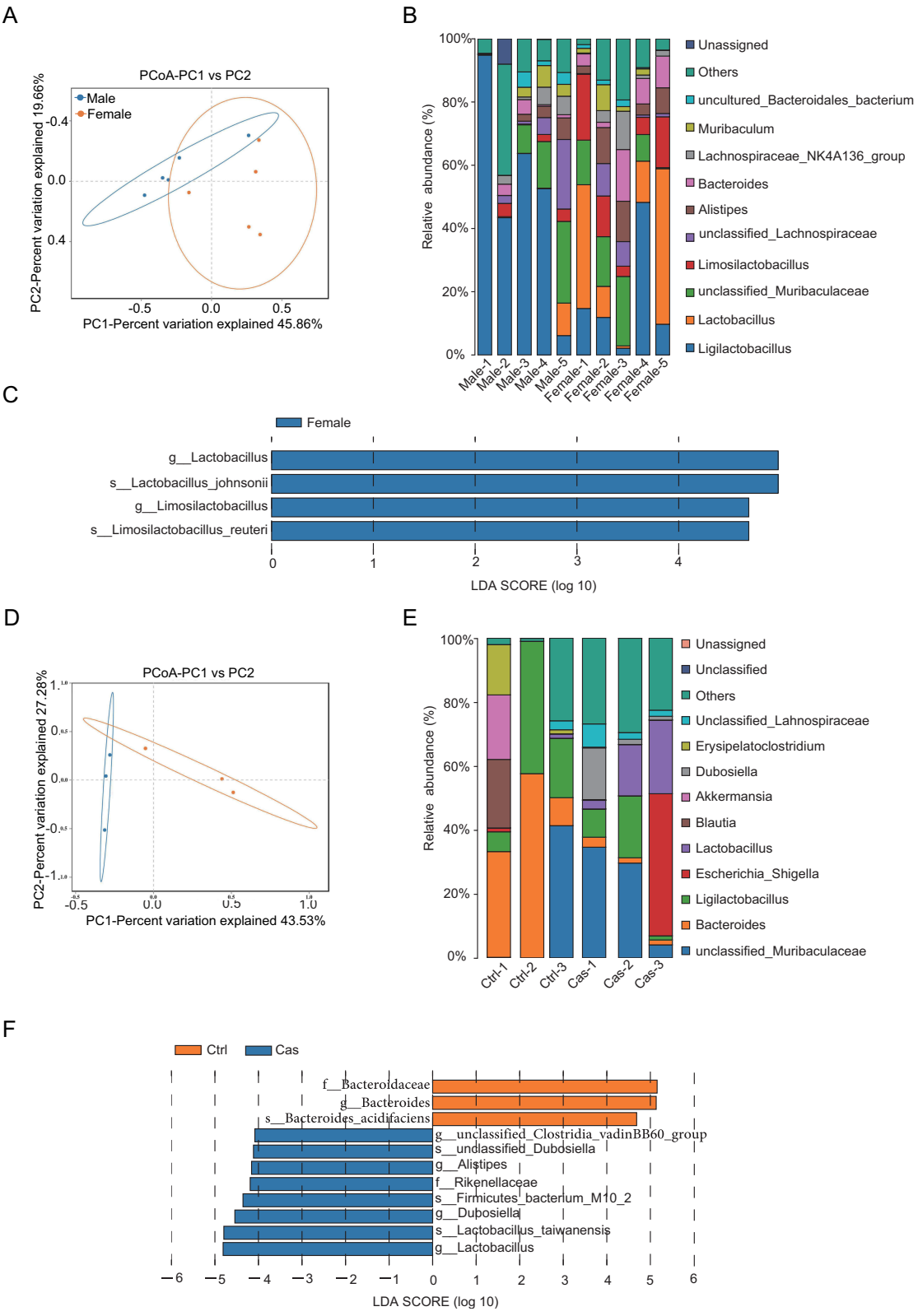

Figure 3 Impact of sex factors on the gut microbiota composition in SKG mouse model of arthritis. (**A**) PCoA of microbial composition based on Bray Curtis for female (n=5) and male (n=5) SKG mice (*P-value* = 0.009, permutational multivariate analysis of variance (PERMANOVA) by Adonis). (**B**) Genus-level taxonomic composition in female and male SKG model mice, shown as a stacked bar plot. (**C**) LEfSe analysis was applied. The bar chart length represents the contribution of differential species (ie, LDA Score). Strains with significantly different abundances between female and male SKG mice are displayed (LDA Score≥4). (**D**) PCoA of microbial composition based on Bray-Curtis dissimilarity in sham-operated (n=3) and castrated (n=3) male SKG mice (p value = 0.01, PERMANOVA by Adonis). (**E**) Genus-level taxonomic composition in sham-operated and castrated male SKG mice, shown as a stacked bar plot (**F**) LEfSe analysis between sham-operated and castrated male SKG mice (LDA Score≥4).

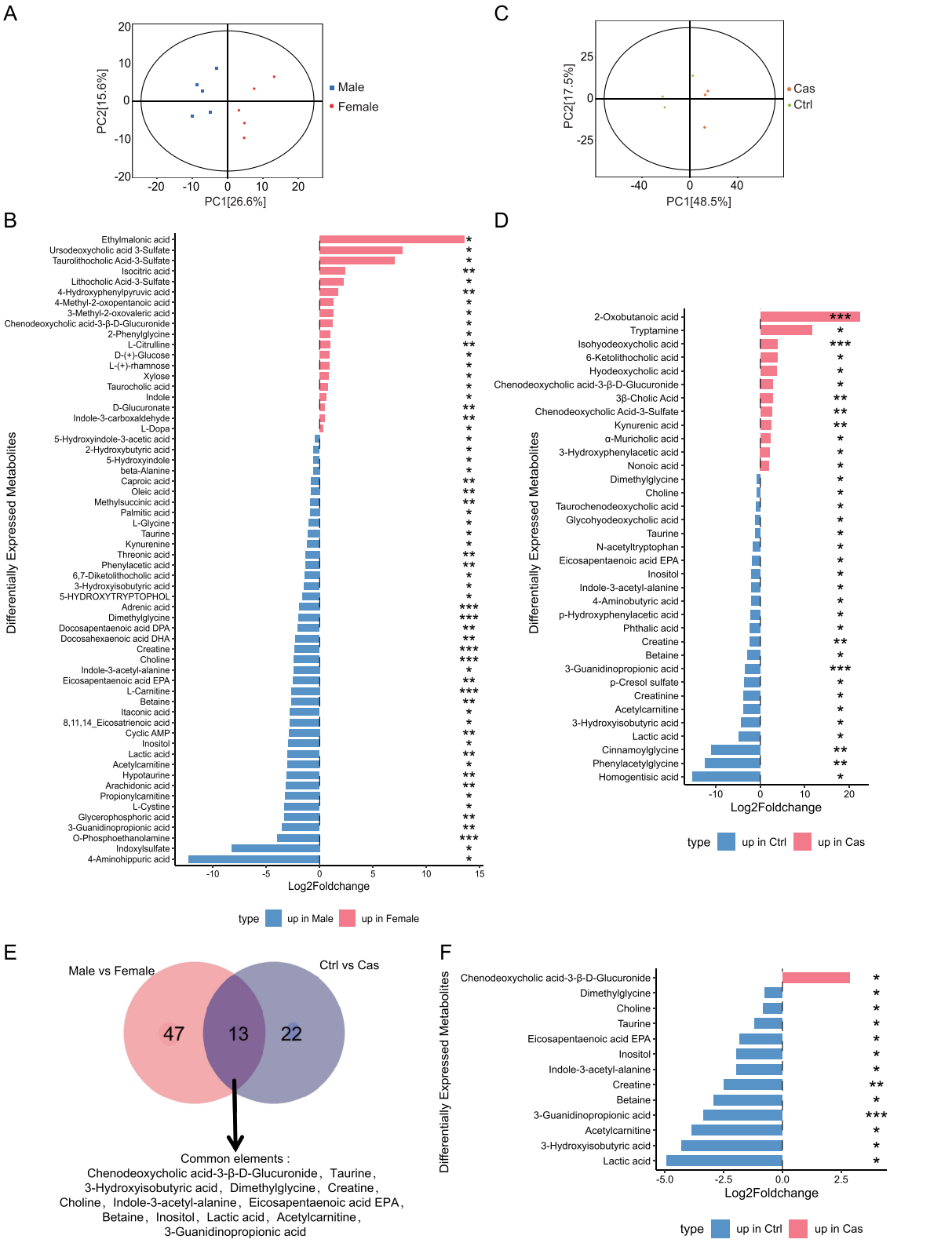

Figure 4 Influence of sex factors on gut metabolites in SKG model of arthritis. (**A**) PCA of intestinal metabolites in female (n=5) and male (n=5) SKG mice model. (**B**) Metabolites with differential expression were ranked according to the $\log_2$ fold - change between female and male SKG mice. (**C**) PCA of intestinal metabolites in sham-operated (n=3) and castrated (n=3) male SKG mice. (**D**) Metabolites with differential expression were ranked according to the $\log_2$ fold - change between sham-operated and castrated male SKG mice. (**E**) Intersection analysis of differential metabolites identified in (**B** and **D**). (**F**) Thirteen differential metabolites enriched and ranked by $\log_2$ fold-change between sham-operated and castrated male SKG mice. *p < 0.05, **p < 0.01, ***p< 0.001.

https://doi.org/10.2147/JIR.S552491

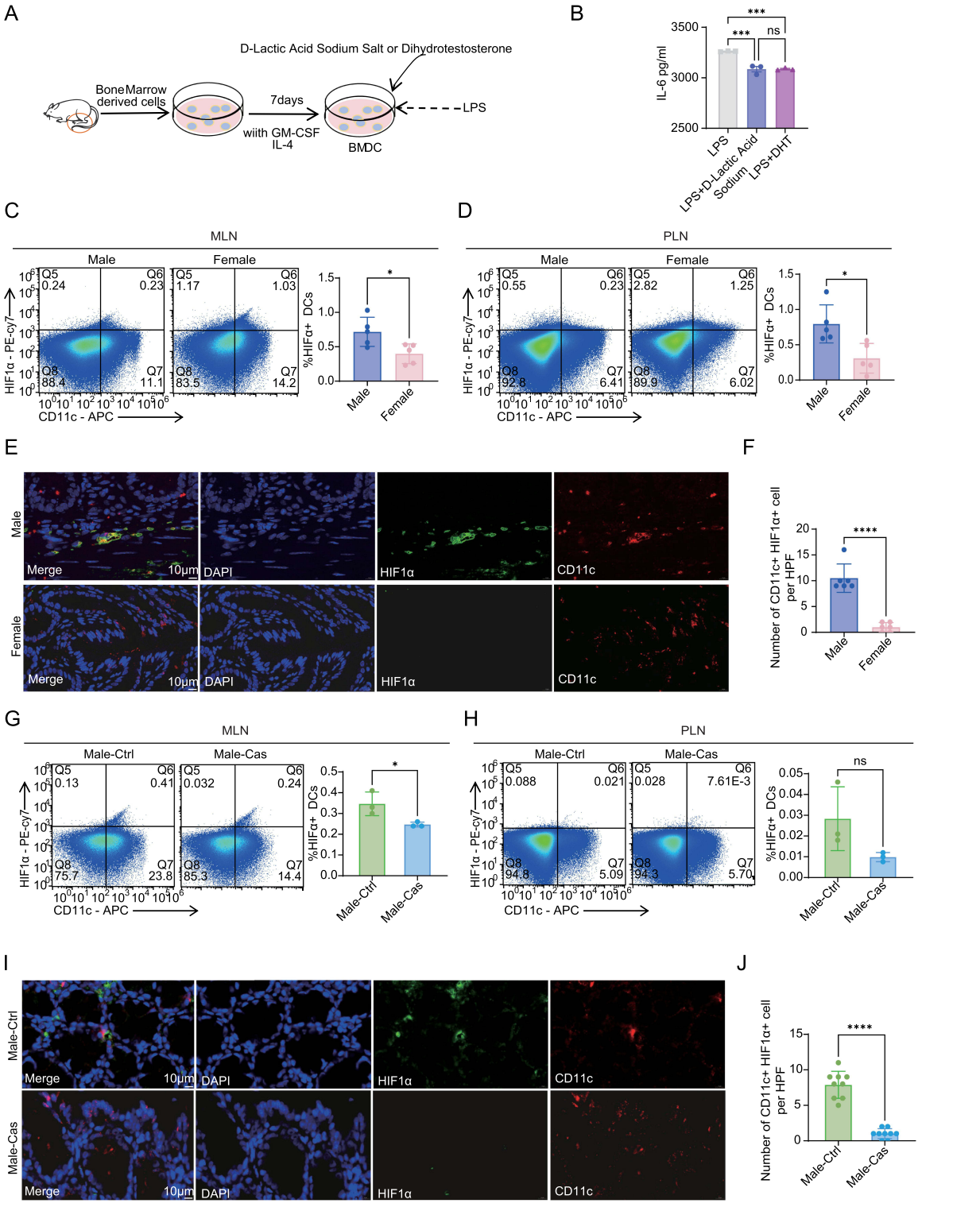

Figure 5 Androgen regulated HIF1α expression in DC cells. (**A**) Schematic diagram of BMDC cell experiment, and the Orange circle marks the mouse tibiofibular region used for the isolation of BMDCs. (**B**) ELISA was used to detect the secretion of IL-6 from LPS-stimulated BMDCs after the addition of D-lactic acid sodium or DHT. (**C** and **D**) Flow cytometry analysis and quantification of HIF1α+ DCs (CD11c+) in the MLN (**C**) and PLN (**D**) of female (n=5) and male (n=5) SKG mice. (**E**) Immunofluorescence staining for CD11c (red) and HIF1α (green) in colorectal tissues of female (n=3) and male (n=3) SKG mice model. Cell nuclei were counterstained with DAPI (blue) (Scale bar=10μm). (**F**)The total count of CD11c+ HIF1α+ cells per high-power field (HPF) was calculated. (**G** and **H**) Flow cytometry analysis and quantification of HIF1α+ DCs (CD11c+) in the MLN (**G**) and PLN (**H**) of sham-operated (n=3) and castrated (n=3) SKG mice. (**I**) Immunofluorescence staining for CD11c (red) and HIF1α (green) in colorectal tissues of sham-operated (n=3) and castrated (n=3) SKG mice. Cell nuclei were counterstained with DAPI (blue) (Scale bar=10μm). (**J**)The total count of CD11c+ HIF1α+ cells per HPF. Error bars indicate mean ± SD for (**B–D, F–H** and **J**). Statistical significance was determined using the Student's *t*-test. *P < 0.05, ***P < 0.001, ****P ≪0.0001.

Abbreviation: ns, not significant.

autoimmune encephalomyelitis (EAE) model, which inhibits proinflammatory cytokine expression in DCs.[24] Therefore, we investigated whether lactate influences HIF1α expression in DCs in the SKG arthritis model. Flow cytometry analyzed MLN and PLN from male and female SKG mice. Female SKG mice exhibited a lower proportion of HIF1α + DCs in MLN compared to males, with analogous differences in PLN (Figure 5C and D). Immunofluorescence co-localization staining revealed that the expression of HIF1α in CD11c+ cells was upregulated in male mice compared to females (Figures 5E and F). Flow cytometry of MLN and PLN in castrated versus sham-operated male SKG mice showed a decreased proportion of HIF1α+ DCs in castrated MLN, with a similar trend in PLN compared to control male mice (Figure 5G and H). Immunofluorescence co-localization staining of intestinal tissues indicated that the expression of HIF1α in CD11c+ cells was reduced in castrated males compared to sham-operated males, consistent with their lower intestinal lactate levels (Figure 5I and J).

These data demonstrate that both lactate and androgens reduce proinflammatory factor secretion by LPS-stimulated BMDCs. Fluctuations in CD11c+HIF1α+ cells correlate with intestinal lactate level changes. Androgens and lactate promote an immune tolerance phenotype in mucosal DCs in the SKG arthritis model.

Discussion

In this study, we investigated the role of sex differences and androgen regulation in shaping immune responses, gut microbiota, and metabolic profiles in the SKG mouse model of arthritis. Our findings indicate that sex and androgen regulation influence gut metabolites and immune responses, especially in terms of DC subsets, which are crucial for immune tolerance and inflammation regulation.

Our research findings indicate that female SKG model mice have higher disease activity scores, more pronounced joint swelling, and more significant inflammatory infiltration in joint and intestinal tissues compared to male mice. These results are consistent with previous research conducted by Rosenzweig's group.[25] Notably, we observed sex-based differences in the distribution of immune cells within lymph nodes. Female mice had a significant increase in cDC2 in the MLN, while male mice showed an increase in cDC1 cells in intestinal-and joint-related lymph nodes. In the male SKG mouse model, androgen deprivation exacerbates the arthritis phenotype, a finding consistent with the research by Rebecca C. Keith.[26] Her study demonstrated that testosterone deficiency increases the prevalence and severity of arthritis in SKG mice, yet the specific mechanism remains unreported.

Our work further investigates the role of androgens in the development of arthritis in SKG mice. When comparing sham-operated male SKG mice with 4-week-old castrated male SKG mice, the number of cDC1 cells in the MLN and PLN of the sham-operated group was significantly reduced. This suggests that androgens might play a crucial role in regulating immune tolerance. Previous studies have demonstrated that the expression of CD103 in cDC1 can promote the tolerance of intestinal FoxP3+CD8+Tregs.[27] This implies a potential link between the elevated cDC1 expression in the MLN of male mice and immune tolerance in the arthritis mouse model. Additionally, previous ovariectomy experiments on 7 to 8-week-old female SKG mice have shown that estrogen can alleviate the symptoms of spondyloarthritis in these mice.[28,29] Given that mice of this age may have reached sexual maturity, and the potential influence of estrogen cannot be ruled out, further in-depth investigation into the impact of sex hormones on arthritis induction in SKG mice is warranted.

In addition to immune cell composition, we examined the gut microbiota and metabolites in male and female SKG mice. Our analysis revealed significant sex-related differences in microbial composition, with female mice and castrated male mice exhibiting higher abundances of Lactobacillus. This discovery holds significance as past research has linked high levels of Lactobacillus to arthritis disease activity.[30] Moreover, exploring how androgen regulates gut microbiota warrants further investigation in the future.

In vitro experiments demonstrated that androgens or D-lactic acid sodium exert effects on LPS-stimulated BMDCs, lowering levels of the proinflammatory cytokine IL-6. This indicates that androgens directly inhibit proinflammatory DC responses, a finding warranting further investigation. Consistent with earlier notes, androgens modulate microbial alterations and levels of lactate, and our findings confirm that D-lactic acid sodium reduces secretion of the proinflammatory cytokine IL-6 by DCs. Reduced HIF1α+ DCs in MLN and PLN of castrated male mice further support the hypothesis that androgens regulate the immune tolerance of DCs in the SKG arthritis model. These

findings align with previous studies, which show that lactate activates HIF1α in DCs and limits DC proinflammatory in EAE model.[24]

In conclusion, our findings provide evidence that sex hormones and androgen modulate immune tolerance in arthritis through regulation of gut microbiota, lactate metabolism and cDC1 cells. For clinical applications, understanding the role of sex hormones and microbiota in arthritis could lead to significant advancements in future treatment strategies. Androgens, as modulators of immune tolerance, may offer a novel therapeutic approach for female RA patients. For instance, testosterone supplementation or androgen receptor agonists could help regulate gut microbiota, lactate metabolism and enhance the function of cDC1 cells. Moreover, interventions targeting the gut microbiota, such as the use of Lactobacillus antagonists or promoting anti-inflammatory microbial species, could serve as effective complementary strategy. Therefore, future research should further explore the role of androgens and gut microbiota in the immune system, particularly how precision, sex-specific interventions can regulate immune tolerance and immune-inflammatory responses.

Limitations

This study explored the influence of sex disparities and androgen regulation on the gut microbiota, metabolic traits, and immune response in the SKG mouse model of arthritis and the male castration model. Although the mouse model provides valuable mechanistic insights, it remains important to investigate the relationship between sex, gut microbiota, lactate derived from the microbiota, and mucosal cell phenotypes in arthritis patients. Further studies are needed to validate these findings, laying the foundation for future clinical and microbiota-targeted therapies.

Data Sharing Statement

The datasets and materials generated and/or analyzed during the current study are available from the corresponding author, Lingjuan Jiang, at irisjlj@163.com, upon reasonable request.

Ethics Approval and Consent to Participate

All animal experiments were approved by the Animal Ethics Committee of Peking Union Medical College Hospital. The animal ethics committee approval number is XHDW-2023-054. The welfare of experimental animals complies with the guidelines specified in Laboratory Animal - Guideline for Ethical Review of Animal Welfare, policy number is GB/T 35892-2018.

Acknowledgments

We acknowledge the Animal Facility of Peking Union Medical College Hospital for providing the facilities for animal housing and a SPF environment, and the Biomarker Discovery and Validation Facility for providing experimental sites and equipment.

Author Contributions

All authors made a significant contribution to the work reported, whether that is in the conception, study design, execution, acquisition of data, analysis and interpretation, or in all these areas; took part in drafting, revising or critically reviewing the article; gave final approval of the version to be published; have agreed on the journal to which the article has been submitted; and agree to be accountable for all aspects of the work.

Funding

This work was funded by National Natural Science Foundation of China (No. 82471837); CAMS Innovation Fund for Medical Sciences (No. 2021-I2M-1-016), and Peking Union Medical College Hospital Talent Cultivation Program (Category D, UHB11899).

Disclosure

The authors declare that they have no competing interests in this work.

References

1. Gravallese EM, Firestein GS. Rheumatoid arthritis - common origins, divergent mechanisms. *N Engl J Med*. 2023;388(6):529–542. doi:10.1056/NEJMra2103726
2. Yang DD, Krasnova A, Nead KT, et al. Androgen deprivation therapy and risk of rheumatoid arthritis in patients with localized prostate cancer. *Ann Oncol*. 2018;29(2):386–391. doi:10.1093/annonc/mdx744
3. Chakraborty B, Byemerwa J, Krebs T, Lim F, Chang C-Y, McDonnell DP. Estrogen receptor signaling in the immune system. *Endocr Rev*. 2023;44(1):117–141. doi:10.1210/endrev/bnac017
4. Zhang X, Zhong H, Li Y, et al. Sex- and age-related trajectories of the adult human gut microbiota shared across populations of different ethnicities. *Nat Aging*. 2021;1(1):87–100. doi:10.1038/s43587-020-00014-2
5. Markle JGM, Frank DN, Mortin-Toth S, et al. Sex differences in the gut microbiome drive hormone-dependent regulation of autoimmunity. *Science*. 2013;339(6123):1084–1088. doi:10.1126/science.1233521
6. Rogers GB. Germs and joints: the contribution of the human microbiome to rheumatoid arthritis. *Nat Med*. 2015;21(8):839–841. doi:10.1038/nm.3916
7. Zhang X, Chen B-D, Zhao L-D, Li H. The gut microbiota: emerging evidence in autoimmune diseases. *Trends Mol Med*. 2020;26(9):862–873. doi:10.1016/j.molmed.2020.04.001
8. Zaiss MM, Joyce Wu H-J, Mauro D, Schett G, Ciccia F. The gut-joint axis in rheumatoid arthritis. *Nat Rev Rheumatol*. 2021;17(4):224–237. doi:10.1038/s41584-021-00585-3
9. Jiang L, Shang M, Yu S, et al. A high-fiber diet synergizes with Prevotella copri and exacerbates rheumatoid arthritis. *Cell Mol Immunol*. 2022;19(12):1414–1424. doi:10.1038/s41423-022-00934-6
10. Kayama H, Okumura R, Takeda K. Interaction between the microbiota, epithelia, and immune cells in the intestine. *Annu Rev Immunol*. 2020;38:23–48. doi:10.1146/annurev-immunol-070119-115104
11. Michaudel C, Sokol H. The gut microbiota at the service of immunometabolism. *Cell Metab*. 2020;32(4):514–523. doi:10.1016/j.cmet.2020.09.004
12. Spivak I, Fluhr L, Elinav E. Local and systemic effects of microbiome-derived metabolites. *EMBO Rep*. 2022;23(10):e55664. doi:10.15252/embr.202255664
13. Liu L, Chen G, Liu J, et al. Sequential production of secondary metabolites by one operon affects interspecies interactions in *Enterobacter* sp. CGMCC 5087. *Innov Life*. 2023;1(2):100023. doi:10.59717/j.xinn-life.2023.100023
14. Verbunt J, Stassen FRM. Probiotic membrane vesicles: emerging tools for disease treatment. *Microbiome Res Rep*. 2025;4(2):25. doi:10.20517/mrr.2025.20
15. Miyauchi E, Shimokawa C, Steimle A, Desai MS, Ohno H. The impact of the gut microbiome on extra-intestinal autoimmune diseases. *Nat Rev Immunol*. 2023;23(1):9–23. doi:10.1038/s41577-022-00727-y
16. Galván-Peña S, Zhu Y, Hanna BS, Mathis D, Benoist C. A dynamic atlas of immunocyte migration from the gut. *Sci Immunol*. 2024;9(91):eadi0672. doi:10.1126/sciimmunol.adi0672
17. MacDonald L, Elmesmari A, Somma D, et al. Synovial tissue myeloid dendritic cell subsets exhibit distinct tissue-niche localization and function in health and rheumatoid arthritis. *Immunity*. 2024;57(12):2843–2862. doi:10.1016/j.immuni.2024.11.004
18. Rehaume LM, Mondot S, Aguirre de Cárcer D, et al. ZAP-70 genotype disrupts the relationship between microbiota and host, leading to spondyloarthritis and ileitis in SKG mice. *Arthritis Rheumatol*. 2014;66(10):2780–2792. doi:10.1002/art.38773
19. Wirtz S, Popp V, Kindermann M, et al. Chemically induced mouse models of acute and chronic intestinal inflammation. *Nat Protoc*. 2017;12(7):1295–1309. doi:10.1038/nprot.2017.044
20. Gargaro M, Scalisi G, Manni G, et al. Indoleamine 2,3-dioxygenase 1 activation in mature cDC1 promotes tolerogenic education of inflammatory cDC2 via metabolic communication. *Immunity*. 2022;55(6):1032–1050. doi:10.1016/j.immuni.2022.05.013
21. Nii T, Maeda Y, Motooka D, et al. Genomic repertoires linked with pathogenic potency of arthritogenic Prevotella copri isolated from the gut of patients with rheumatoid arthritis. *Ann Rheumatic Dis*. 2023;82(5):621–629. doi:10.1136/ard-2022-222881
22. Li F, Xing X, Jin Q, et al. Sex differences orchestrated by androgens at single-cell resolution. *Nature*. 2024;629(8010):193–200. doi:10.1038/s41586-024-07291-6
23. Qi X, Yun C, Pang Y, Qiao J. The impact of the gut microbiota on the reproductive and metabolic endocrine system. *Gut Microbes*. 2021;13(1):1894070. doi:10.1080/19490976.2021.1894070
24. Sanmarco LM, Rone JM, Polonio CM, et al. Lactate limits CNS autoimmunity by stabilizing HIF-1α in dendritic cells. *Nature*. 2023;620(7975):881–889. doi:10.1038/s41586-023-06409-6
25. Lee EJ, Vance EE, Brown BR, et al. Investigation of the relationship between the onset of arthritis and uveitis in genetically predisposed SKG mice. *Arthritis Res Ther*. 2015;17(1):218. doi:10.1186/s13075-015-0725-z
26. Keith RC, Sokolove J, Edelman BL, et al. Testosterone is protective in the sexually dimorphic development of arthritis and lung disease in SKG mice. *Arthritis Rheum*. 2013;65(6):1487–1493. doi:10.1002/art.37943
27. Joeris T, Gomez-Casado C, Holmkvist P, et al. Intestinal cDC1 drive cross-tolerance to epithelial-derived antigen via induction of FoxP3+CD8+ Tregs. *Sci Immunol*. 2021;6(60):eabd3774. doi:10.1126/sciimmunol.abd3774
28. Jeong H, Kim IY, Bae E-K, Jeon CH, Ahn K-S, Cha H-S. Selective estrogen receptor modulator lasofoxifene suppresses spondyloarthritis manifestation and affects characteristics of gut microbiota in zymosan-induced SKG mice. *Sci Rep*. 2021;11(1):11923. doi:10.1038/s41598-021-91320-1
29. Jeong H, Bae E-K, Kim H, et al. Estrogen attenuates the spondyloarthritis manifestations of the SKG arthritis model. *Arthritis Res Ther*. 2017;19(1):198. doi:10.1186/s13075-017-1407-9
30. Zhang X, Zhang D, Jia H, et al. The oral and gut microbiomes are perturbed in rheumatoid arthritis and partly normalized after treatment. *Nat Med*. 2015;21(8):895–905. doi:10.1038/nm.3914